This article has been accepted for publication in a future issue of this journal, but has not been fully edited. Content may change prior to final publication. Citation information: DOI 10.1109/TSG.2017.2762601, IEEE Transactions on Smart Grid

Distributed Control of Inverter-Interfaced Microgrids Based on Consensus Algorithm with Improved Transient Performance

Jiajun Duan, Cheng Wang, Hao Xu, Wenxin Liu, Yaosuo Xue, Jian-Chun Peng, and Hui Jiang

***Abstract*—Conventional control solutions of the inverter-interfaced microgrids are usually designed based on models with fully decoupled subsystems. The negligence of the strong coupling due to power lines impedance leads to large transient line currents, which might trigger false protection. Besides, the droop-based control methods unnecessarily introduce system frequency and voltage deviations. To overcome these issues, a novel distributed control scheme is proposed for the inverter-interfaced microgrids in this paper. The objective of the primary control is to regulate the bus voltages and frequency while suppressing the transient line currents. The objective of secondary control is to maintain fair load sharing. Both primary control and secondary control are distributed and subsystems or control agents only require measurements from local and neighboring subsystems. The detailed control problem formulation, control design and stability analysis are presented in the paper. The effectiveness of the proposed control solution is evaluated through extensive simulations based on both simplified and detailed models.**

***Index Terms*—Inverter-interfaced microgrids, distributed generations, transient line current, feedback linearization.**

I. Introduction

Distributed energy resources or distributed generators (DGs) are the basic building blocks of the emerging microgrid paradigm [1]. Various types of DG such as photovoltaics, wind turbines, energy storages and fuel cells are interfaced to microgrids through power electronic converters/inverters [2]. Besides environmental benefits, the characteristics of fast response speed and high flexibility make these inverter-interfaced DGs preferable in a small-scale power system to the conventional synchronous generators (SG) [3]. However, it is quite challenging to control microgrids comprised of such DGs due to negligible inertia and intermittent generations, together with unexpected load changes. As one of the fundamental elements and resilience tools for the future smart grid, the inverter-interfaced microgrids require more effective control and operation methods that can fully unlock their technical potentials.

Traditional control solutions, which have been proven to be effective for large-scale power systems, cannot be introduced to microgrids directly [4]. There are mainly two types of solutions that can be found in recent research [5-11]. The first category, also the commonly promoted solution, is to increase the "virtual" inertia of the inverter-interfaced microgrids so that microgrids can behave similarly to the traditional power systems [5]. However, these solutions cannot fully unleash the potentials of microgrids in terms of flexibility and response speed. The second category of solutions is to model such microgrids as an integration of decoupled subsystems, where the impacts from neighboring subsystems are simply modeled as measurable disturbances. Then the control problem is formulated as a multi-agent control system. At the lower primary control level, droop and inner cascaded loops of proportional-integral (PI) controls are deployed to track the control references regulated by the upper secondary control level. Since microgrids are modeled similar to that of unmanned vehicle systems that have no physical connections among subsystems, many existing solutions in cooperative control [6-7], optimal control [8-9] and game theory [10-11] can be introduced. In the past years, there are many successful developments along this route. These works definitely promote researches on microgrids controls and help to bridge the gaps among related disciplines, especially controls, power systems, and power electronics [5-11]. However, there are still many open problems that deserve further investigations.

In general, existing solutions that combine traditional primary control and advanced secondary control demonstrate comprised performance associated with several issues in modeling, control objective, and control strategy. First, the line dynamics should not be neglected during the modeling and control design process [12]. Most of the existing distributed control algorithms are based on the microgrid model with fully decoupled subsystems [13-14]. However, the line impedances of microgrids are usually in the same range as the parameters of output filters of DGs [6, 12-13]. Thus, merely ignoring the strong physical coupling to trade for achieving the distributed control design may result in large transient line current that could make the control ineffective and even trigger false protections. Secondly, the conventional control objective is

This work was supported in part by the U.S. Office of Naval Research under Grant No. N00014-16-1-3121, National Natural Science Foundation of China under Grant No. 51477104, and Shenzhen International Cooperation Research Project under Grant No. GJHZ20150313093836007.

Jiajun Duan is with the Department of Electrical and Computer Engineering, Lehigh University, Bethlehem, PA 18015 USA (e-mail: jid213@lehigh.edu).

Hao Xu is with the Department of Electrical & Biomedical Engineering, University of Nevada, Reno, NV 89557 USA (e-maill: haoxu@unr.edu).

Wenxin Liu is with the Department of Electrical and Computer Engineering, Lehigh University, Bethlehem, PA 18015 USA (e-mail: wel814@lehigh.edu).

Yaosuo Xue is with Oak Ridge National Laboratory, Oak Ridge, TN 37831, USA (e-mail: xuey@ornl.gov).

Jian-Chun Peng is with the College of Mechatronics and Control Engineering, Shenzhen University, Shenzhen 518060, China (e-mail: jcpeng@szu.edu.cn).

Hui Jiang is with the College of Optoelectronic Engineering, Shenzhen University, Shenzhen 518060, China (e-mail: huijiang@szu.edu.cn).

1949-3053 (c) 2017 IEEE. Personal use is permitted, but republication/redistribution requires IEEE permission. See http://www.ieee.org/publications_standards/publications/rights/index.html for more information.

This article has been accepted for publication in a future issue of this journal, but has not been fully edited. Content may change prior to final publication. Citation information: DOI 10.1109/TSG.2017.2762601, IEEE Transactions on Smart Grid

always focused on regulating the capacitor voltage on the *LCL* output filters instead of the bus voltage where the loads are connected. Since the bus voltage is not under control directly, a small voltage deviation is unavoidable, which is undesired for the loads. Third, the droop-based primary control unnecessarily introduces the frequency deviations to the system [14]. For the conventional synchronous generator, there is a link between the electrical frequency and the mechanical rotating speed. However, such relationship does not exist in the inverter-interfaced DGs.

In order to better address the aforementioned challenges, several important factors have to be reconsidered for control design. Once the line impedances/dynamics are taken into the consideration during the control design, a microgrid can no longer be treated as an integration of fully decoupled subsystems. To improve the transient line currents performance of the interconnected subsystems, the basic communication among each control agent is necessary. The establishment of communication network renders the primary control not decentralized (communication-free) anymore. In fact, even though the conventional droop-based control methods are claimed to be decentralized, the centralized or inter-agent communications have been unavoidably used during the reference frame transformation as well as system frequency synchronization [12-14]. It has been demonstrated that moderate amount of inter-agent communications can greatly improve the control performance by introducing certain global situational awareness [15]. With the rapid development of communication technologies, preference should not merely be given to the decentralized control designs. On the contrary, an appropriate balance should be evaluated between the control performance and the communication requirement.

In this paper, a distributed control solution is presented for microgrids consisting of multiple inverter-interfaced DGs. The LC output filters are applied so that the bus voltages can be directly managed. Both secondary and primary control schemes are developed to better coordinate the different requirements of system performance from the perspectives of both customers (frequency and voltage) and utilities (efficiency and reliability). At the upper control level, power generation references (*P* and *Q*) are obtained by a distributed consensus-based load sharing algorithm. Then the power generation references are used to calculate the phase angle references of bus voltages through DC power flow. At the primary control level, the phase angle references are used to decide the direct and quadrature (*dq*) components of bus voltage references. Besides, it has been demonstrated that the line currents are directly impacted by the dynamic responses of bus voltages. According to this theoretical basis, a consensus-based primary controller is designed, which not only realizes the accurate voltage regulation but also suppresses the transient line currents significantly. The contributions of this paper are summarized as follows.

1. Both secondary and primary control problems of AC microgrids are reformulated. The control objectives of utilities and customers are well coordinated according to the requirements of the system performance.
2. Based on the dynamic model of the system, the relationship between line current and bus voltage has been analyzed. It is proven that the transient line current can be reduced if the local controls of bus voltages are coordinated.
3. Based on the analysis, a distributed secondary controller is designed to realize the fair load sharing and a distributed primary controller is also developed to balance the voltage regulation and transient line current suppression, respectively. The distributed solution can increase the reliability and flexibility of the system comparing to the centralized control.
4. Finally, extensive simulations are performed with switch-level and different scale microgrid models (including traditional synchronous generator). The simulation results demonstrate the effectiveness of the proposed control solution.

The rest of the paper is organized as follows. Section II introduces the formulation of the microgrids control problem. Section III presents the designs of the primary and secondary control. Section IV provides the simulation results with both simplified numerical microgrids model and detailed switch-level microgrids models. Section V provides the concluding remarks and discusses the future work.

II. Formulation of Microgrids Control Problem

Without loss of generality, the single-line schematic diagram of a microgrid consisted of three DGs with *LC*-filters is shown in the Fig. 1. For each DG, the intermediate or direct output of a distributed renewable or a traditional energy resource is represented by a DC source, and then connected to a voltage source inverter (VSI). Then, an LC-filter is utilized after VSI for harmonic current filtering and voltage stabilization [16]. Each DG may or may not have a load directly connected to its output filter/bus. Multiple subsystems consisted of inverter-interfaced DGs and loads are connected together through and power lines to form an integral mesh-type microgrid.

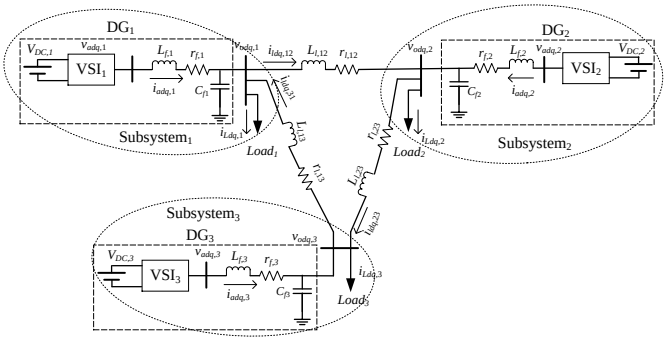

Fig. 1. Schematic diagram of an inverter-interfaced microgrid.

Due to the fast response of power converters, the transient dynamics of the system are actually dominated by the *RLC* components of output filter and power lines. Therefore, an averaging model, which considers these dynamic responses, is more suitable for the control design than a detailed switching model. On the other hand, a detailed switching model can be used to simulate and evaluate the effectiveness of the proposed

1949-3053 (c) 2017 IEEE. Personal use is permitted, but republication/redistribution requires IEEE permission. See http://www.ieee.org/publications_standards/publications/rights/index.html for more information.

This article has been accepted for publication in a future issue of this journal, but has not been fully edited. Content may change prior to final publication. Citation information: DOI 10.1109/TSG.2017.2762601, IEEE Transactions on Smart Grid

controller. The system model used in control design is summarized as follows.

The state equations dominating the *LC*-filter dynamics for i^{th} inverter can be expressed as

$$\dot{i}_{ad,i} = -\frac{1}{L_{f,i}}(r_{f,i}i_{ad,i} + v_{od,i}) + \omega_n i_{aq,i} + \frac{1}{L_{f,i}}v_{ad,i} \quad (1)$$

$$\dot{i}_{aq,i} = -\frac{1}{L_{f,i}}(r_{f,i}i_{aq,i} + v_{oq,i}) - \omega_n i_{ad,i} + \frac{1}{L_{f,i}}v_{aq,i} \quad (2)$$

$$\dot{v}_{od,i} = \frac{1}{C_{fi}}(i_{ad,i} - i_{ld,i} - i_{Ld,i}) + \omega_n v_{oqi} \quad (3)$$

$$\dot{v}_{oq,i} = \frac{1}{C_{fi}}(i_{aq,i} - i_{lq,i} - i_{Lq,i}) - \omega_n v_{od,i} \quad (4)$$

where $L_{f,i}$ is the inductance of *L*-filter; $r_{f,i}$ is the parasitic resistances of the inductor; ω_n is the nominal electrical angular velocity; $v_{od,i}$ and $v_{oqi,}$ are *dq*-components of the load bus voltage of the i^{th} subsystem ($v_{o,i}$); and $v_{ad,i}$ and $v_{aq,i}$ are the *dq*-components of the output voltage of i^{th} DG ($v_{a,i}$). $i_{ld,i} = \sum_{j=1}^{n_i} i_{ld,ij}$ and $i_{lq,i} = \sum_{j=1}^{n_i} i_{lq,ij}$ are the *dq*-components of the overall line current leaving bus #*i* ($i_{ldq,i}$) with n_i being the number of buses connected to bus #*i*; $i_{Ld,i}$ and $i_{Lq,i}$ are the *dq*-components of load current at bus #*i* ($i_{L,i}$).

Assuming that a power line is connecting bus #*i* and bus #*j*, its dynamics can be represented as

$$\dot{i}_{ld,ij} = \frac{1}{L_{l,ij}}(-r_{l,ij}i_{ld,ij} + v_{od,i} - v_{od,j}) + \omega_n i_{lq,ij} \quad (5)$$

$$\dot{i}_{lq,ij} = \frac{1}{L_{l,ij}}(-r_{l,ij}i_{lq,ij} + v_{oq,i} - v_{oq,j}) - \omega_n i_{ld,ij} \quad (6)$$

where $r_{l,ij}$ represents the resistance of the power line linking buses *i* and *j*; $L_{l,ij}$ is the lumped inductance of the power line; and $i_{ld,ij}$ and $i_{lq,ij}$ are the *dq*-components of line current ($i_{l,ij}$).

Equations (1-6) represent the formulation of one subsystem as shown in Fig. 1. Each subsystem is assigned to one control agent. A completed microgrid model is consisted of any number of such subsystems and can be represented as a multi-agent system. The model (1-6) can represent a general category of microgrids in which loads are directly connected to the DG terminal buses instead of intermediate buses. The above linear modelling system can result in a nonlinear control problem if the control objective is to regulate quantities which are formulated as nonlinear functions of system states, e.g., output voltage ($v_{o,i}$), line current ($i_{l,ij}$) and active power.

Basically, each subsystem is established on its own *dq*-reference frame. Thus, a common reference frame is necessary to integrate multiple subsystem models together. The common reference is a signal that can be represented as $\cos(\omega t+\theta)$, and there are two ways to decide it for the system. The first method is to take the dynamic measurements of one DG as the system-wide reference [13]. The second method is to generate a common reference signal by an accurate clock or function generator. Both methods require the communication network to spread the common reference signals to the recipients either in a centralized way or in a distributed way.

Since the frequency of the reference DG oscillates throughout the time, the first method cannot avoid introducing disturbances to the phase locked loop (PLL) measurements. Thus, the dynamics of PLL have to be considered in the first method, which unnecessarily increases the difficulties of control design. In contrast, the second method takes use of a reference signal with a constant frequency. Because all of DGs share the same reference information, PLL can be saved in the second method. It not only minimizes the frequency oscillations by setting a constant frequency reference (e.g., 60 Hz), but also simplifies the control design and implementation process.

Additionally, a power system usually considers four control performance indices, i.e., active power generation (*P*), reactive power generation (*Q*), bus voltage (*V*), and system frequency (*f*). In general, *V* and *f* are more important to the loads, while utilities care more about *P* and *Q*. Ideally, these four indices are equally important for a power system to operate effectively and efficiently. However, it is challenging and even impossible to achieve the perfect control of all quantities simultaneously due to the complex relationship and conflicts among them. Based on system characteristics and operation requirements, four indices (*P*, *Q*, *V* and *f*) should be carefully selected and prioritized during the control design.

III. Control Design For Inverter Interfaced Microgrids

Generally, microgrids normally adopt two different control modes, i.e., *V-f* control and *P-Q* control, which target different concerns or operating conditions [17, 20]. In SG-based large-scale power systems, the predefined droop characteristics are usually deployed to counteract the impacts of unavoidable load change and reference setting inaccuracy [4, 14]. Since rotor speed of an SG can reflect the charge or discharge of its mechanical potential energy during the supply-demand imbalance, which is further linked to its electrical frequency, using *P-f* droop control is necessary and reasonable. However, the inverter-interfaced DG does not have such physical *P-f* coupling due to the decoupling of DC source and AC generation. Since the frequency of the invertor-interfaced DG can be easily maintained, using droop control to adjust frequency reference during system operating change unnecessarily increases the frequency oscillations. Moreover, multiple frequency signals will be detected in the system during the transient stages if each subsystem adjusts its frequency reference separately. It not only disrupts the convergence of PLL, and also increases difficulties for frequency evaluation.

Based on above introduction, it is logical to infer that the solution should have two control levels for larger time-scale and real-time coordination of subsystems, respectively. The upper-level secondary control is in charge of control reference setting while the lower-level primary control is responsible for control reference adjustment and tracking. This way of control implementation differs from the conventional control solutions, but it becomes more effective to realize certain specific control objectives. In order to guarantee fast and smooth tracking of the control references, and avoid a surge of line current, a novel control algorithm needs to be designed. The control strategy has to be thoughtful of the priority of control objectives while trying to keep flexibility and efficiency.

In the proposed control design, the primary control objective is load bus voltage (*V*) regulations, and the secondary control

1949-3053 (c) 2017 IEEE. Personal use is permitted, but republication/redistribution requires IEEE permission. See http://www.ieee.org/publications_standards/publications/rights/index.html for more information.

This article has been accepted for publication in a future issue of this journal, but has not been fully edited. Content may change prior to final publication. Citation information: DOI 10.1109/TSG.2017.2762601, IEEE Transactions on Smart Grid

objective is fair load-sharing (*P*). The reference of frequency *f* is set to be a constant, and the reactive power *Q* is not directly regulated. For the reference set of bus voltage, the root mean square (RMS) value is fixed and only phase angle is adjusted. The adjustment of the voltage phase angle is based on the consideration of both fair load-sharing and complexity of uncertain operating conditions. In this way, the critical quantities (i.e., *V* and *f*) can be well regulated together. Details of the proposed control solution are presented in the following subsections.

A. Secondary Control Design

The objective of secondary control is to find the phase angle references (δ_i^*) of the bus voltages (V_o) based on the operational constraints of fair load sharing in a two-step procedure. First, a distributed consensus-based algorithm presented in [18] is used to decide generation references of the DGs ($P_{G,i}^*$). Second, the generation references ($P_{G,i}^*$) and the desired bus voltage (V_o^*) are applied to calculate the bus phase angel references (δ_i^*). The two-step secondary control design are introduced as follows.

According to [18], the control objective of fair load sharing is to assign the power generation of each DG based on a common utilization level K_u, which is decided by the overall demand $\sum P_L$ and the overall maximum generation capability $\sum P_{max}$. The overall demand includes the total demands of loads and the estimated system-wide losses. The overall maximum generation is determined by the predicted generation of the intermittent sources and the physical limitation of the non-intermittent sources. Since the consensus algorithm can find the global average value of the distributed signals, it can be used to find the average demand and average maximum generation through distributed communications. Once these two quantities are obtained by the control agents, the local utilization levels can be calculated, which is same for the entire system. Thus, the fair load sharing can be achieved by synchronizing the utilization level and the impact of inaccurate generation prediction can be minimized as well.

In order to realize the desired load sharing, the corresponding references of voltage phase angles (δ_i^*) have to be determined through power flow analysis based on the generation references ($P_{G,i}^*$). The DG with the maximum generation capability can be selected as the slack bus, while others can be considered as PV buses. Either AC or DC power flow can be utilized to solve δ_i^* in a distributed manner as introduced in [19]. Since a slight inaccuracy is not as important as the response speed, the DC power flow becomes the preferable choice and is used in this paper. Besides, considering that the DC power flow can be achieved within the predetermined steps (time), it can help to realize more timely control reference updating for large-scale microgrids.

B. Primary Control Design

The reference setting from secondary control cannot immediately become available for the primary control due to the computation and communication delay. It can be regarded as a small disturbance for the system and is neglected in this paper. Once the voltage phase angles references δ_i^* are decided, the *dq*-components of the bus voltage references $v_{od,i}^*$ and $v_{oq,i}^*$ can be calculated according to (7).

$$\begin{cases} v_{od,i}^* = V_{o,i}^* \cos(\delta_i^*) \\ v_{oq,i}^* = V_{o,i}^* \sin(\delta_i^*) \end{cases} \tag{7}$$

where $V_{o,i}^*$ is the RMS voltage reference at bus *i*. By tracking the control references ($v_{od,i}^*$, $v_{oq,i}^*$, and f^*=60 Hz), the primary control objectives (*V*-*f* regulation) can be achieved and the secondary control objectives ($P_{G,i}^*$) can also be approached.

The developed primary control targets bus voltage regulation while suppressing the transient line current with the upmost efforts. Before proceeding, the relationship between line currents and bus voltage is analyzed first. The coordinated control design is then developed based on the theoretic basis.

a) Transient line current suppression

Most of existing primary control algorithms for microgrids have no consideration of the transient line currents. Similar to most upper-level secondary control algorithms, which can only address the steady-state constraints in line currents periodically at a large time-scale [6, 13]. The unexpected transient line current surge raises the challenges to tune the protection system and may cause big losses due to the false action of protection devices. Therefore, when the primary controller is conducting the major control objectives of regulating the *V* and *f*, it should also be capable of suppressing the transient line current surge as much as possible. To ensure the transient line current limitation is satisfied, the Lyapunov stability analysis can be used to relate the line current $i_{l,ij}$ with output voltage $v_{o,i}$. Recall the linear dynamic (5) and (6), they can be rewritten as

$$\dot{i}_{ldq,ij} = A_{l,ij} i_{dq,ij} + e_{vdq,ij} \tag{8}$$

where

$$i_{ldq,ij} = \begin{bmatrix} i_{ld,ij} \\ i_{lq,ij} \end{bmatrix},\ e_{vdq,ij} = \begin{bmatrix} v_{odi} - v_{odj} \\ v_{oqi} - v_{oqj} \end{bmatrix},\ A_{l,ij} = \begin{bmatrix} -\dfrac{r_{l,ij}}{L_{l,ij}} & \omega_n \\ -\omega_n & -\dfrac{r_{l,ij}}{L_{l,ij}} \end{bmatrix}.$$

Next, if selecting Lyapunov function candidate as $H(i_{ldq,ij}) = \frac{1}{2} i_{ldq,ij}^T i_{ldq,ij}$, the first derivative of the Lyapunov function candidate can be represented as

$$\dot{H}(i_{ldq,ij}) = \frac{1}{2} \dot{i}_{ldq,ij}^T i_{ldq,ij} + \frac{1}{2} i_{ldq,ij}^T \dot{i}_{ldq,ij} \tag{9}$$

Substituting (8) into (9), one can have

$$\begin{aligned} \dot{H}(i_{ldq,ij}) &= \frac{1}{2} i_{ldq,ij}^T (A_{l,ij} i_{dq,ij} + e_{vdq,ij}) + \frac{1}{2} (A_{l,ij} i_{dq,ij} + e_{vdq,ij})^T i_{ldq,ij} \\ &= \frac{1}{2} i_{ldq,ij}^T (A_{l,ij} + A_{l,ij}^T) i_{dq,ij} + \frac{1}{2} i_{ldq,ij}^T e_{vdq,ij} + \frac{1}{2} e_{vdq,ij}^T i_{dq,ij} \\ &\le -\frac{1}{3} \frac{r_{l,ij}}{L_{l,ij}} \left\| i_{l,ij} \right\|^2 + \frac{3L_{l,ij}}{r_{l,ij}} \left\| e_{vdq,ij} \right\|^2 \end{aligned} \tag{10}$$

Assuming that the line currents need to be bounded as $\|i_{ldq,ij}\| \le i_{lB,ij}$, the line current constraint can be transferred into the bound of $e_{vdq,ij}$ based on the Lyapunov stability analysis as,

$$\left\| e_{vdq,ij} \right\| \le \frac{1}{3} \frac{r_{l,ij}}{L_{l,ij}} i_{lB,ij} \tag{11}$$

Note that the definition of $e_{vdq,ij}$ is the potential voltage difference between bus #*i* and bus #*j*. Therefore, equation (11)

1949-3053 (c) 2017 IEEE. Personal use is permitted, but republication/redistribution requires IEEE permission. See http://www.ieee.org/publications_standards/publications/rights/index.html for more information.

This article has been accepted for publication in a future issue of this journal, but has not been fully edited. Content may change prior to final publication. Citation information: DOI 10.1109/TSG.2017.2762601, IEEE Transactions on Smart Grid

implies that the transient line currents can be suppressed if the terminal voltages (v_{oi} and v_{oj}) are converging along the same trajectory consistently. In this way, the $\|e_{vdq,ij}\|$ can be minimized with the transient line currents being suppressed significantly at the same time. Based on the above theoretical analysis, a consensus-based primary controller is designed in the next subsection. The output voltages are designed to converge in a consistent manner to suppress the transient line current.

b) Bus voltage regulation

To better regulate the bus voltages, a two-step feedback linearization based control algorithm is designed. According to (7), the tracking error of bus voltage can be defined as

$$\begin{cases} e_{vod,i} = v_{od,i} - v_{od,i}^{*} \\ e_{voq,i} = v_{oq,i} - v_{oq,i}^{*} \end{cases} \tag{12}$$

Since $v_{od,i}^{*}$ and $v_{oq,i}^{*}$ are updated periodically, they can be treated as constants between control updating intervals. Based on (3) and (4), the dynamics of voltage tracking errors can be reformulated as

$$\begin{cases} \dot{e}_{vod,i} = f(e_{vod,i}) + B_{vod,i} i_{ad,i} \\ \dot{e}_{voq,i} = f(e_{voq,i}) + B_{voq,i} i_{aq,i} \end{cases} \tag{13}$$

where $f\left(e_{vod,i}\right) = \frac{1}{C_{fi}}(-i_{ld,i} - i_{Ld,i}) + \omega_n v_{oqi}$, $B_{vod,i} = B_{voq,i} = \frac{1}{C_{f,i}}$ and $f\left(e_{voq,i}\right) = \frac{1}{C_{fi}}(-i_{lq,i} - i_{Lq,i}) - \omega_n v_{od,i}$. Then, using the feedback linearization technique, the voltage tracking controller can be derived as

$$\begin{cases} i_{adi}^{*} = B_{od,i}^{-1}\left\{\left[-f(e_{vod,i}) - K_{vd} e_{vod,i}\right] + \sum_j^n a_{ij}\left(e_{vod,i} - e_{vod,j}\right)\right\} \\ i_{aqi}^{*} = B_{oq,i}^{-1}\left\{\left[-f(e_{voq,i}) - K_{vq} e_{voq,i}\right] + \sum_j^n a_{ij}\left(e_{voq,i} - e_{voq,j}\right)\right\} \end{cases} \tag{14}$$

where K_{vd} and K_{vq} are positive control gains. n_i is the total number of DGs. a_{ij} is the coefficient of the information exchanged between agent #i and agent #j.

Based on a rigorous stability analysis, all of the voltage tracking errors will converge to the same value (i.e., zero) as long as the coefficients a_{ij} satisfy certain constraints [6-7]. The consensus items in (14) make sure that the output voltage of different DGs ($e_{vdq,ij}$) converge in a consistent way, which is able to greatly decrease the surge of transient line currents. Next, targeting tracking of the *LC* filter current references i_{adi}^{*} and i_{aqi}^{*}, the current tracking errors can be attained as

$$\begin{cases} e_{iad,i} = i_{ad,i} - i_{ad,i}^{*} \\ e_{iaq,i} = i_{aq,i} - i_{aq,i}^{*} \end{cases} \tag{15}$$

The corresponding dynamics of the current tracking errors are

$$\begin{cases} \dot{e}_{iad,i} = \dot{i}_{ad,i} - \dot{i}_{ad,i}^{*} = f(e_{iad,i}) + B_{iad,i} v_{ad,i} \\ \dot{e}_{iaq,i} = \dot{i}_{aq,i} - \dot{i}_{aq,i}^{*} = f(e_{iaq,i}) + B_{iaq,i} v_{aq,i} \end{cases} \tag{16}$$

where $f\left(e_{iad,i}\right) = \frac{1}{L_{f1}}(-r_{fi} i_{adi} - v_{odi}) + \omega_n i_{aqi} - \dot{i}_{ad,i}^{*}$, $B_{iad,i} = B_{iaq,i} = \frac{1}{L_{f,i}}$ and $f\left(e_{iaq,i}\right) = \frac{1}{L_{fi}}(-r_{fi} i_{aqi} - v_{oqi}) - \omega_n i_{adi} - \dot{i}_{aq,i}^{*}$.

Then the practical control input can be designed as

$$\begin{cases} v_{ad,i} = B_{iad,i}^{-1}\left[-f(e_{iad,i}) - K_{id} e_{iad,i}\right] \\ v_{aq,i} = B_{iaq,i}^{-1}\left[-f(e_{iaq,i}) - K_{iq} e_{iaq,i}\right] \end{cases} \tag{17}$$

where K_{id} and K_{iq} are positive control gains.

The above design follows the similar procedure of other general feedback linearization based control algorithms that developed for microgrids [13]. The differences are with the control formulation (control model and control objectives) as well as the consideration of transient line currents. The flowchart shown in Fig. 2 illustrates how measurements and control input/output are transmitted and applied by the proposed control scheme. It is important to note that the algorithm is distributed in the sense that signals for subsystem control computation are all locally measured.

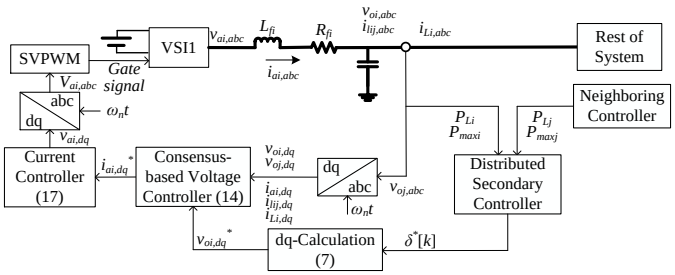

Fig. 2. The flowchart of the control solution

C. Control Implementation

The overall implementation diagram of the proposed control scheme is presented in Fig. 3. During the initialization of the consensus-based load sharing algorithm, each agent estimates the local load and the maximum generation of the corresponding DG. Through the distributed communications among the agents, the synchronized utilization level can be found. Thus, the power generation reference of each subsystem can be calculated locally. Then, the phase angle references of the bus voltages can be calculated using power generation references, bus voltage settings, and system admittance matrix. The detailed secondary control process can be found in [18-19] and will be omitted in this paper to avoid the redundancy. The distributed operation also requires the direct interactions of subsystem agents. Finally, the *dq*-components of the bus voltage references are determined by the RMS value of bus voltages together with its adjusted phase angle references.

During the regulation process, the control objective is to make the bus voltages tracking the corresponding references while suppressing the line currents. Based on a predefined common reference frame rotating at a constant frequency (60 Hz), the common phase angle reference can be found by the integration of frequency (ωt). Due to the fast response speed of inverter-interfaced DGs, tracking of frequency reference can be realized in an instant time. Thus, each control agent can convert the *dq*-components of the control signals to *abc*-components via the common information of the phase angle reference. Finally, PWM signals are generated based on the final control signals for the inverters.

1949-3053 (c) 2017 IEEE. Personal use is permitted, but republication/redistribution requires IEEE permission. See http://www.ieee.org/publications_standards/publications/rights/index.html for more information.

This article has been accepted for publication in a future issue of this journal, but has not been fully edited. Content may change prior to final publication. Citation information: DOI 10.1109/TSG.2017.2762601, IEEE Transactions on Smart Grid

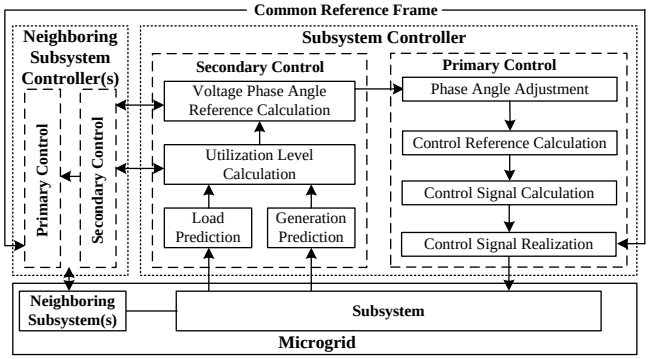

Fig. 3. Flow chart diagram of the proposed microgrid control scheme.

IV. Simulation Results

In order to comprehensively evaluate the performance of the proposed control solution, simulations are performed on both mathematical model and the detailed switch-level model using Matlab/Simulink. The detailed switch-level model is much more complicated than the mathematical model represented in (1-6) which makes it capable of testing the proposed solution under uncertain model dynamics. Parameters of a 3-DG microgrid model and control gains are provided in Table I, which is modified based on [12]. The proposed solution is also compared with conventional proportion-integration (PI) based primary control algorithm [12] through simulation.

TABLE I: PARAMETERS OF MICROGRID

Parameter	Value	Description
r_{f1}, r_{f2}, r_{f3}	0.50, 0.51, 0.52 Ω	Filter resistance
L_{f1}, L_{f2}, L_{f3}	4.21, 4.20, 4.215 *mH*	Filter inductance
C_{f1}, C_{f2}, C_{f3}	20, 20, 20 *uf*	Filter inductance
r_{l12}, r_{l23}, r_{l31}	0.151, 0.152, 0.154 Ω	Line resistance
L_{l12}, L_{l23}, L_{l31}	0.42, 0.41, 0.414 *mH*	Line inductance
K_{vd} , K_{vq}	250	Control gain
K_{id}, K_{iq}	25	Control gain
ω_n	377 *rad/s*	Nominal angular velocity
T_s	10^{-4} *s*	Sampling time

A. Simulation with Mathematical Microgrid Model

During the primary control algorithm test, maximum generations are held fixed and a step change of constant load is simulated. Implementation details of the secondary control algorithms can be found in the referenced paper [18]. In this case, the secondary control algorithm is only activated once at the instant of time of load change.

The simulation starts from the steady state and a step load change is simulated at 0.5s. The maximum generations of three generator references are 0.9, 0.8, 1.0 per unit (*pu*), respectively and held constant during the 2.5-second simulation. Three active power loads before and after the load change are 0.51, 0.51, 0.60 *pu* and 0.61, 0.51, 0.60 *pu*, respectively. The initial generation references are 0.54, 0.48, 0.60 *pu*, which is obtained based on the estimated maximum generations. Based on DC power flow and the RMS voltage settings of 1.0, 1.0, 1.0 *pu*, the phase angles reference before load change are 0.006, 0.08, 0.0002 *rad*. Under this simulation setting, the generation reference and voltage phase angle references after load change are 0.58, 0.51, 0.64 *pu* and 0.001, 0.008, 0.06 *rad*, respectively.

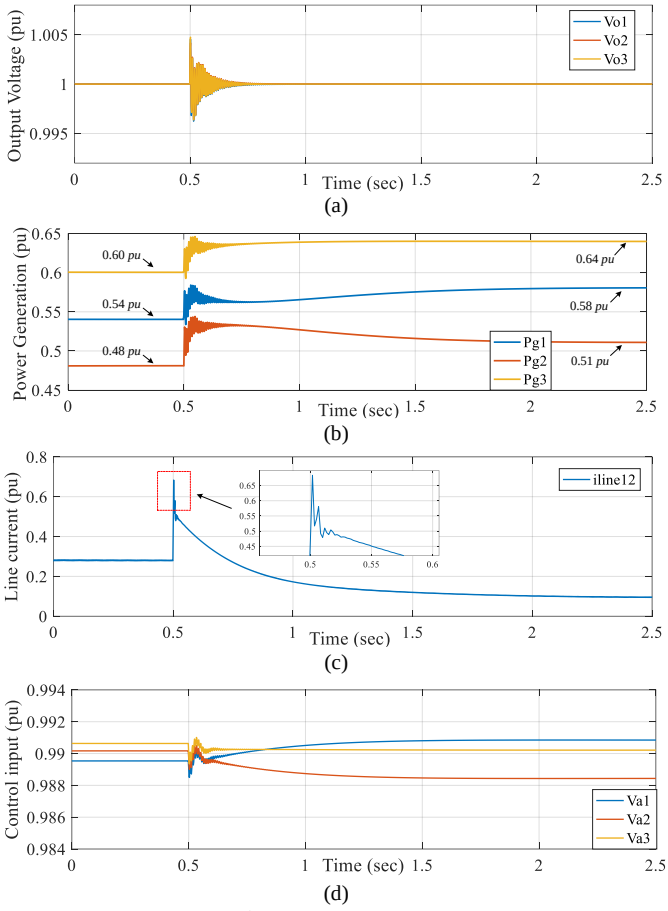

Fig. 4. Simulation results of PI-based control scheme: (a). Load bus voltages (v_o); (b). Power generation (P_G); (c). Line current (i_l). (d). control inputs (v_a).

First, the PI-based controller presented in [12] is applied. The PI gains have been well-tuned using the classical Ziegler-Nichols method [21], and the PI gains of voltage and current controller are shown in Table II. Since the PI controller has no global situational awareness, it is very difficult to tune the appropriate gains of PI controllers to satisfy both local (bus voltage) and system-level (line currents) requirements of microgrids. The corresponding responses of load bus voltages v_o and power generation P_G of DGs are presented in Fig. 4(a) and Fig. 4(b), respectively. As can be observed, both v_o and P_G are able to track their references before and after the load changes. The convergence of the reactive power demonstrated that the developed secondary control can also work together with the conventional primary control. In Fig. 4(c), a large line current surge (at $line_{12}$) can be observed at the beginning of load change. The overshoot is during the transient stage over 0.65 *pu*, which might lead certain troubles to the protection system. In addition, both power generation and line current take a quite long time to converge due to the interaction of each subsystem. Therefore, the only control objective of voltage regulation for the conventional controllers greatly limits their performance. The overall control inputs are given in Fig. 4(d).

TABLE II: PARAMETERS OF PI CONTROLLER

	Voltage controller	Current controller
P gain	0.50	1.00
I gain	10.0	25.0

1949-3053 (c) 2017 IEEE. Personal use is permitted, but republication/redistribution requires IEEE permission. See http://www.ieee.org/publications_standards/publications/rights/index.html for more information.

This article has been accepted for publication in a future issue of this journal, but has not been fully edited. Content may change prior to final publication. Citation information: DOI 10.1109/TSG.2017.2762601, IEEE Transactions on Smart Grid

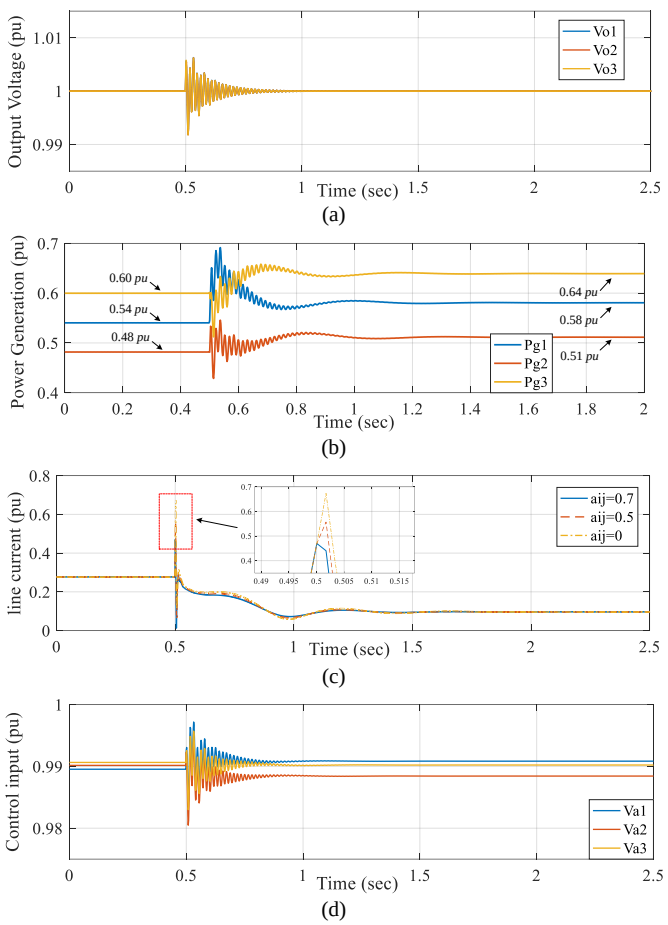

Fig. 5. Simulation results of the proposed control scheme: (a). Load bus voltages (vo); (b). Power generation (PG); (c). Line current (i_i); and (d). control signals.

Next, the proposed controller is used under the same loading conditions. The responses of bus voltage, power generation, line current, and control signals are shown in the four plots of Fig. 5, respectively. It can be noticed that both voltages and power generations are able to track their corresponding references. In addition, the surge currents on the power lines get significantly suppressed. As can be seen in the zoomed-in subplot of Fig. 5 (c), different consensus weight a_{ij} can reduce the transient line current surge to the distinct degrees. The overshoot of the transient line current is similar to the PI-based controller if a_{ij} =0, which means no consensus component is included in the primary control. But it can be reduced under 0.5 *pu* when a_{ij} =0.7. A comparison analysis of transient line current and bus voltage of using different control parameters are given in Table III. From simulation results, one can see that the overshoot of bus voltage just increases by 0.3% while the line current overshoot can be reduced as much as 20%. Since the improved control over line currents means a wider range of operating conditions and less faulty triggering of the protection system, the performance improvement is considered to be significant and the slight compromise over voltage regulation is worthful.

TABLE III: THE CONTROL PERFORMANCE COMPARISON RESULTS

PI controller	
Max. mag. of transient line current	Max. mag. of transient bus voltage
0.68 pu	0.005 pu
Proposed controller	
Consensus Weight a_{ij}	Max. mag. of transient line current	Max. mag. of transient bus voltage
0.3	0.67 pu	0.008 pu
0.5	0.56 pu	0.008 pu
0.7	0.47 pu	0.008 pu
0.9	0.46 pu	0.008 pu
1.0	0.46 pu	0.008 pu

By comparing Fig. 4(b) and Fig. 5(b), one can see that the power generations converge differently. The consensus-based primary controller not only suppresses the line current surge, but also accelerates the converging speed of the power generations. The control inputs are shown in the Fig. 5(d). It is true that the control inputs of the proposed controller have more severe changes compared with the PI controller. Therefore, it is necessary to evaluate whether such control inputs can be realized by the practical power inverters. In the next subsection, the proposed control algorithm is tested on a detailed switch-level model.

B. Simulation with Detailed 6-DG Microgrid Model

In this case, a larger-scale detailed microgrid model shown in Fig. 6 is used to evaluate the performance of the proposed control algorithm. More details are considered in the switching level model, such as the PWM, 2-level inverter and *dq-abc* transformations. This system consists of 6 DGs including 5 inverter-interfaced DGs and 1 SG. For the inverter-interfaced DGs, the proposed secondary/primary control method is used as in the previous cases. For the SG, a detailed genset model from Simscape Power Systems toolbox is applied including a turbine governor, an automatic voltage regulator, an exciter, and a power system stabilizer. Since this work is mainly focused on the inverter-interfaced microgrid control, only small percentage of generation from the SG is tested and the dynamic coordination problem of two different generation units is neglected. In order to better test the effectiveness of the proposed control algorithm, different line parameters given in Table IV are used [12]. The rest of system settings are same as the previous cases.

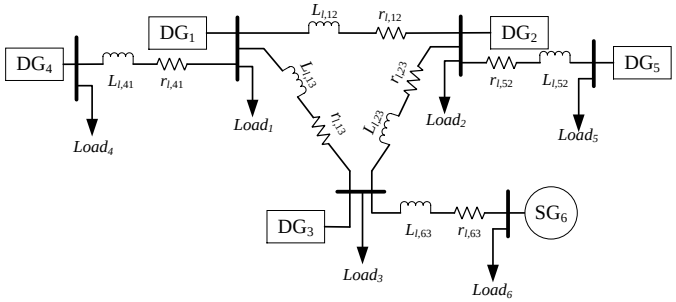

Fig. 6. The topology of a 6-DG microgrid.

TABLE IV: PARAMETERS OF MICROGRID

Parameter	Value
r_{l12}, r_{l23}, r_{l31}, r_{l41}, r_{l52}, r_{l63}	0.15, 0.16, 0.14, 0.17, 0.10, 0.20 Ω
L_{l12}, L_{l23}, L_{l31}, L_{l41}, L_{l52}, L_{l63}	0.42, 0.35, 0.30, 0.45, 0.4, 0.41 *mH*

In order to better evaluate the effectiveness of the proposed control algorithm, a series of load changes including sudden and smooth load changes are conducted. At time 0.5 s, $load_1$ has a step change from 0.75 pu to 0.85 pu. Then, from time 1.5 s to 2.5 s, $load_2$ has a ramp up change from 0.52 pu to 0.60 pu. The overall load consumption of each subsystem is measured and

1949-3053 (c) 2017 IEEE. Personal use is permitted, but republication/redistribution requires IEEE permission. See http://www.ieee.org/publications_standards/publications/rights/index.html for more information.

This article has been accepted for publication in a future issue of this journal, but has not been fully edited. Content may change prior to final publication. Citation information: DOI 10.1109/TSG.2017.2762601, IEEE Transactions on Smart Grid

shown in Fig. 7, and the maximum generation capacity of each local DG is assumed to be 1 pu, 0.8 pu, 0.8 pu, 0.6 pu, 0.6 pu and 0.2 pu. Based on the local load measurement and the predicted power generation, the utilization level shown in Fig. 8(a) is updated every 0.2 s incrementally using the distributed secondary control scheme as described in Section III-A [18-19]. Then, the references of phase angle δ_i^* acquired through the load flow are shown in the Fig. 8(b), which will be used to generate the bus voltage references $v_{od,i}^*$ and $v_{oq,i}^*$ on dq-axis. The fully distributed secondary control process can significantly increase the flexibility and stability of the system. The simulation results of the proposed primary controller are shown in the Fig. 9. As can be seen from Fig. 9(a) and Fig. 9(b), both system frequency and bus voltage can track the corresponding references well. Finally, the line current between DG_1 and DG_2 is shown in the Fig. 9(c). Similar to the previous cases, the proposed control algorithm can effectively suppress the transient line current. Throughout the studies, the effectiveness of the proposed controller is verified.

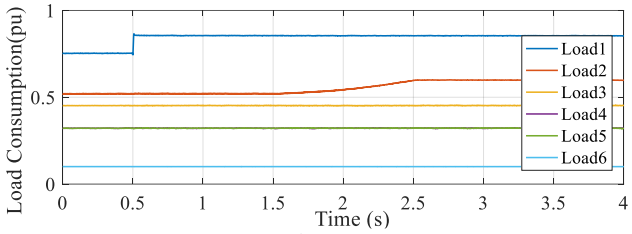

Fig. 7. Load consumption change of each subsystem.

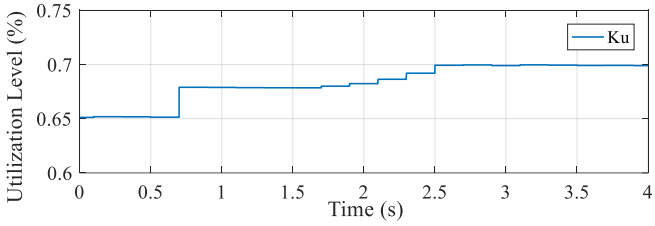

(a)

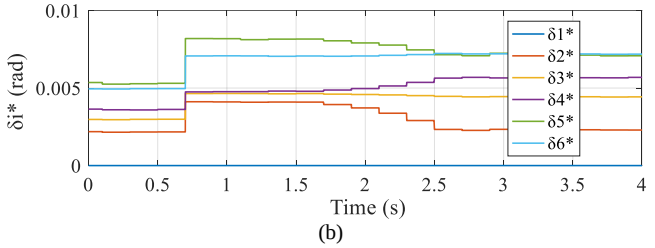

(b)

Fig. 8. Evaluation of the secondary control: (a). Utilization level (%) of each DG; (b) Phase angle references δ_i^*.

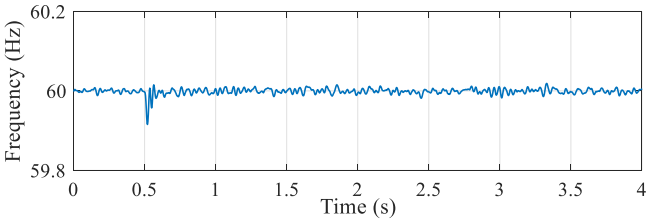

(a)

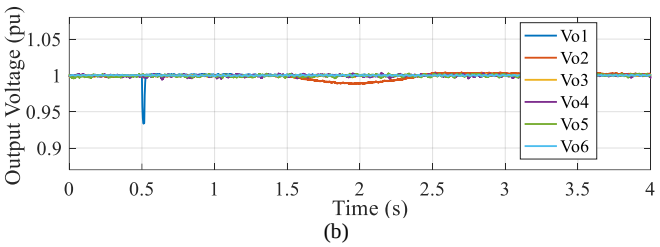

(b)

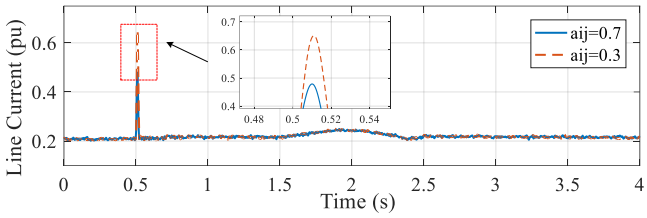

(c)

Fig. 9. Simulation results of the proposed control scheme on 6-DG microgrid: (a). System frequency (f); (b). Load bus voltages (v_o); (c). Line current (i_{ij}).

V. Concluding Remarks

Inverter-interfaced microgrids are difficult to control due to the fast dynamics, uncertainties, and a wide range of operating conditions. The conventional control solutions cannot fully utilize the advantages of the power electronic system and would result in unnecessary voltage and frequency deviations as well as large overshoot on the transient line current. In this paper, the relationship between bus voltages and line currents is analyzed. Based on this theoretical analysis, the proposed control solution can not only realize desired voltage and frequency regulation and also suppress the transient line current. The effectiveness of the proposed control solution has been demonstrated through extensive simulations. For the simulated cases, the proposed controller can effectively reduce the transient line current as much as 20% while the transient voltage response is only slightly compromised. Future work includes designing advanced control algorithms, addressing cyber uncertainties, and testing control solutions through hardware experimentation.

VI. References

[1] J. Rocabert, A. Luna, F. Blaabjerg and P. Rodriguez, “Control of power converters in AC microgrids,” *IEEE Transactions on Power Electronics*, vol. 27, no. 11, pp. 3353-3358, 2012.

[2] Y. Li, D. M. Vilathgamuwa, and P. C. Loh, “Design, analysis and real-time testing of controller for multibus microgrid system,” *IEEE Transactions on Power Electronics*, vol. 19, no. 5, pp. 1195-1204, 2004.

[3] N. Pogaku, M. Prodanovic, and T. C. Green, “Modeling, analysis and testing of autonomous operation of an inverter-based microgrid,” *IEEE Transactions on Power Electronics*, vol. 22, no. 5, pp. 613-625, 2007.

[4] D. Shi , Y. Luo , R. K. Sharma, "Active synchronization control for microgrid reconnection after islanding," in *Innovative Smart Grid Technologies Conference Europe*, Istanbul, Turkey, pp. 1-6, 2014.

[5] J. Zhao, and X. Lyu, “Coordinated microgrid frequency regulation based on DFIG variable coefficient using virtual inertia and primary frequency control,” *IEEE Transactions on Energy Conversion*, vol. 31, no. 3, pp. 833-845, 2016.

[6] H. Cai, G. Hu, F. L. Lewis, and A. Davoudi, “A distributed feedforward approach to Cooperative control of AC microgrid,” *IEEE Transactions on Power Systems*, vol. 31, no. 5, pp. 4057-4067, 2016.

[7] D. He, D. Shi, and R. Sharma, “Consensus-based distributed cooperative control for microgrid voltage regulation and reactive power sharing,” in *IEEE PES Innovative Smart Grid Technologies, Europe*, pp. 1-6, 2014.

1949-3053 (c) 2017 IEEE. Personal use is permitted, but republication/redistribution requires IEEE permission. See http://www.ieee.org/publications_standards/publications/rights/index.html for more information.

This article has been accepted for publication in a future issue of this journal, but has not been fully edited. Content may change prior to final publication. Citation information: DOI 10.1109/TSG.2017.2762601, IEEE Transactions on Smart Grid

[8] H. Xin, Y. Liu, Z. Qu, and D. Gan, "Distributed estimation and control for optimal dispatch of photovoltaic generations, " *IEEE Transactions on Energy Conversion*, vol.29, no.4, pp.988-996, 2014.
[9] A. Maknouninejad, Z. Qu, F. Lewis, and A. Davoudi, "Optimal, nonlinear, and distributed designs of droop controls for DC microgrid," *IEEE Transactions on Smart Grid*, vol.5, no.5, pp.2508-2616, 2014.
[10] V. Nasirian, M. Modares, F. Lewis, and A. Davoudi , "Active loads of a microgrid as players in a differential game," in *IEEE 7th International Symposium on Resilient Control Systems*, 2015, pp. 1-6.
[11] L. Fan, V. Nasirian, H. Modares, F. Lewis, Y. D. Song, and A. Davoudi, "Game-theoretic control of active loads in DC microgrids," *IEEE Transaction on Energy Conversion*, vol. 31, no. 3, pp. 882-895, 2016.
[12] M. Rasheduzzaman, J. A. Mueller, and J. W. Kimball, "An accurate small-signal model of inverter dominated islanded microgrids using dq reference frame," *EEE Journal of Emerging and Selected Topics in Power Electronics*, vol. 2, no. 4, pp. 1070-1080, 2014.
[13] A. Bidram, A. Davoudi, F. L. Lewis, and J. M. Guerrero, "Distributed cooperative secondary control of microgrids using feedback linearization," *IEEE Transactions on Power Systems*, vol. 28, no. 3, pp. 3462-3470, 2013.
[14] V. Nasirian, Q. Shafiee, J. M. Guerrero, and F. L. Lewis, and A. Davoudi, "Droop-free distributed control for AC microgrid," *IEEE Transactions on Power Electronics*, vol. 31, no. 2, pp. 1600-1617, 2016.
[15] K. S. Narendra and S. Mukhopadhyay, "To Communicate or Not to Communicate: A Decision-Theoretic Approach to Decentralized Adaptive Control," in *2010 American Control Conference Marriott Waterfront*, Baltimore, USA, pp. 6369-6376, 2010.
[16] L. Zhou, Y. Chen, A. Luo, J. M. Guerrero, and X. Zhou, "Robust two degrees-of-freedom single-current control strategy for LCL-type grid-connected DG system under grid-frequency fluctuation and grid-impedance variation," *IET Power Electronics*, pp, 1-19, 2016.
[17] W. Guo, L. Mu, and X. Zhang, "Fault models of inverter-interfaced distributed generators within a low-voltage microgrid," *IEEE Transactions on Industrial Electronics*, pp. 1-9, 2016.
[18] W. Zhang, Y. Xu, W, Liu, F. Ferrese, and L. Liu, "Fully distributed coordination of multiple DFIGs in a microgrid for load sharing," *IEEE Transactions on Smart Grid*, vol. 4, no. 2, pp. 806-815, 2013.
[19] W. Zhang, Y. Ma, W, Liu, S. Ranade, and Y. Luo, "Distributed optimal active power dispatch under constraints for smart grids," *IEEE Transactions on Industrial Electronics*, vol. 64, no. 6, pp. 5084-5094, 2017.
[20] Y. Luo , M. Panwar , M. Mohanpurkar , and R. H. Ritwik, "Real time optimal control of supercapacitor operation for frequency response," in *Power and Energy Society General Meeting*, Boston, MA, USA, pp. 1-5, 2016.
[21] F. A. Salem and A. A. Rashed, "PID controllers and algorithms: selection and design techniques applied in mechatronics systems design," *International Journal of Engineering Sciences*, vol. 2, no. 5, pp. 191-203, 2013.

Jiajun Duan (S'2014) was born in Lanzhou, China, in 1990. He received his B.S. degree in Power system and its automation from Sichuan University, Chengdu, China, and M.S. degree in in Electrical Engineering at Lehigh University, Bethlehem, PA in 2013 and 2015, respectively. He is currently pursing the Ph.D. degree at Lehigh University. His research interest includes power system, power electronics, control systems, renewable energy and smart microgrid.

Cheng Wang (S'12) received the B.S. degree in electrical engineering from Southwest Jiaotong University, Chengdu, China in 2011, and is currently working toward the Ph.D. degree in electrical engineering in the School of Electrical and Electronics Engineering, Huazhong University of Science and Technology at Wuhan, China. He is also a research assistant with the Department of Electrical and Computer Engineering, Lehigh University at PA, USA. His research interests include Microgrids, high penetrative grid-interactive photovoltaic system, modular multilevel converters and uninterrupted power systems.

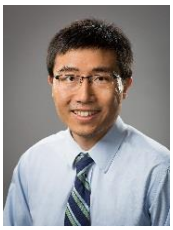

Hao Xu (M'12) was born in Nanjing, China. He received the master's degree in electrical engineering from Southeast University, Nanjing, in 2009, and the Ph.D. degree from the Missouri University of Science and Technology, Rolla, MO, USA, in 2012. He is currently with University of Nevada, Reno, where he is an Assistant Professor with the Department of Electrical & Biomedical Engineering. His current research interests include intelligent control design for advanced power systems, smart grid, autonomous unmanned aircraft systems, and wireless passive sensor network.

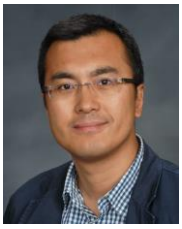

Wenxin Liu (S'01–M'05–SM'14) received the B.S. degree in industrial automation, and the M.S. degree in control theory and applications from Northeastern University, Shenyang, China, in 1996 and 2000, respectively, and the Ph.D. degree in electrical engineering from the Missouri University of Science and Technology (formerly University of Missouri–Rolla), Rolla, MO, USA, in 2005. Currently, he is an Assistant Professor with the Department of Electrical and Computer Engineering, Lehigh University, Bethlehem, PA, USA. His research interests include power systems, power electronics, and controls.

Yaosuo Xue (M'03, SM'12) received the B.Sc. degree in electrical engineering from East China Jiaotong University, Nanchang, China in 1991 and the M.Sc. degree in electrical engineering from the University of New Brunswick, Fredericton, Canada, in 2004. He is currently with Oak Ridge National Laboratory and his research interests include multilevel converters and smart inverter controls for renewable energy and utility applications. He is an Associate Editor of IEEE Transaction on Power Electronics and IEEE Journal of Emerging and Selected Topics in Power Electronics, and technical program co-chairs in several IEEE power electronics conferences.

Jian-Chun Peng (M'04-SM'17) received the B.S. and M.S. degrees from Chongqing University, Chongqing, China, in 1986 and 1989, respectively, and the Ph.D. degree from Hunan University, Hunan, China, in 1998, all in electrical engineering. He is a Professor in Shenzhen University and the director

1949-3053 (c) 2017 IEEE. Personal use is permitted, but republication/redistribution requires IEEE permission. See http://www.ieee.org/publications_standards/publications/rights/index.html for more information.

This article has been accepted for publication in a future issue of this journal, but has not been fully edited. Content may change prior to final publication. Citation information: DOI 10.1109/TSG.2017.2762601, IEEE Transactions on Smart Grid

of the Department of Control Science and Engineering. He was a Visiting Professor from November 2002 to November 2003 at Arizona State University, Tempe, US, and from May 2006 to August 2006, at Brunel University, London, UK. His interests include smart grid optimal operation and control, power electronics application.

Hui Jiang received the B.S. degree from Chongqing University, Chongqing, China, in 1990, and the M.S. and Ph.D. degrees from Hunan University, Hunan, China, in 1999 and 2005, respectively, all in electrical engineering. She is a Professor in Shenzhen University. From November 2005 to November 2006, she was a Visiting Scholar at Brunel University, London, UK. Her interests include power system economics and smart grid operation.

1949-3053 (c) 2017 IEEE. Personal use is permitted, but republication/redistribution requires IEEE permission. See http://www.ieee.org/publications_standards/publications/rights/index.html for more information.